3D Texture Analysis of MRI Relaxation Time Maps for Assessment of Repair Cartilage with Treatment of Allogeneic Human Adipose-Derived Mesenchymal Progenitor Cells

Xinxin Zhao
Shanghai Jiao Tong University School of Medicine Affiliated Renji Hospital
Qing Lu
Shanghai Jiao Tong University School of Medicine Affiliated Renji Hospital
Jingjing Ruan
Shanghai Jiao Tong University School of Medicine Affiliated Renji Hospital
Jia Li
Shanghai Jiao Tong University School of Medicine Affiliated Renji Hospital
Chengxiang Dai
Cellular Biomedicine Group
Mengchao Pei
Chinese Academy of Sciences
Yan Zhou (clare1475@hotmail.com)
Shanghai Jiao Tong University School of Medicine Affiliated Renji Hospital https://orcid.org/0000-0001-9402-1109

Research Article

Keywords: texture analyses, gray level run-length matrix, magnetic resonance relaxation time maps, composition alternations, repair cartilage, human adipose-derived mesenchymal progenitor cells

Posted Date: December 17th, 2021

DOI: https://doi.org/10.21203/rs.3.rs-1157978/v1

Abstract

Background: We used textural analysis matrix to examine the spatial distribution of pixel values and detect the compositional variation of repair cartilage with treatment of allogeneic human adipose-derived mesenchymal progenitor cells (haMPCs).

Methods: Eighteen patients were divided randomly into three groups with intra-articular injections of haMPCs: the low-dose (1.0×10^7 cells), mid-dose (2.0×10^7), and high-dose (5.0×10^7) group with six patients each. 3D texture analyses based on gray level run-length matrix (GLRLM) of the segmented ROIs on MRI relaxation time maps including T1rho, T2, $T2^*$ and $R2^*$. Five GLRLM parameters were analyzed, including run length non-uniformity (RLNonUni), grey level non-uniformity (GLevNonU), long run emphasis (LngREmph), short run emphasis (ShrtREmp) and fraction of image in runs (Fraction). We used the difference before and after treatment (D values) as the object to avoid errors caused by individual differences. Two-tailed Pearson linear correlation analysis was used to investigate correlations between texture parameters and the WOMAC scores.

Results: The heterogeneity of spatial distribution of MRI relaxation time mapping pixels from three groups was decreased to varying degrees at 48 weeks after intra-articular injection of haMPCs. Spatial distribution of cartilage relaxation time maps pixels were uneven and layered, especially in T2 maps. Compared with base time, there were significant differences among three dose groups in GLRLM features for T1rho map including RLNonUni, GLevNonU, LngREmph, for T2 map including LngREmph, GLevNonU, ShrtREmp, for $T2^*$ map including RLNonUni, GLevNonU, and for $R2^*$ map including RLNonUni, GLevNonU. WOMAC pain scores were associated with RLNonUni of T1rho map, GLevNonU of T2 map, LngREmph of $T2^*$ map, LngREmph of $R2^*$ map and Fraction of T1rho map, whereas no significant correlations in other measurements.

Conclusions: MRI texture analysis of cartilage may allow detection of the compositional variation of repair cartilage with treatment of allogeneic haMPCs. This has potential applications in understanding mechanism of stem cells repairing cartilage and assessing response to treatment.

Trial registration: Clinicaltrials, NCT02641860. Registered 3 December 2015.

https://www.clinicaltrials.gov/ct2/show/NCT02641860

1. Introduction

Stem cells have been used to regenerate cartilage defects for decades. Recently, growing evidence suggests therapeutic potential of mesenchymal stem/progenitor cells (MSC/MPC) for cartilage repair and regeneration by their ability to differentiate into chondral tissue [1–3]. The initial change of repair and regenerate occurs at the cellular level, earlier than the gross morphological changes, which can be displayed and quantified by magnetic resonance imaging [4]. The efficacy of intra-articular injection of allogeneic human adipose-derived MPCs (haMPCs) in the knee has been verified in our previous study by multi-compositional magnetic resonance imaging (MRI) methods [5].

MRI provides a novel non-invasive technology to directly visualize cartilage composition associated with osteoarthritis (OA) [6], with its excellent soft tissue contrast and ability to quantify the proteoglycan (PG), glycosaminoglycan (GAG) and collagen fiber network of the extracellular matrix (ECM). Recent advances of MR relaxation time constant mappings, including T1rho, T2, $T2^*$ and $R2^*$, have demonstrated in quantifying these cartilage composition with measurement of mean value in the region of interest (ROI). However, recent cross-sectional [7, 8] and longitudinal [9, 10] studies have shown that subjects with OA have a more heterogeneous distribution of both T2 and T1rho values than controls, demonstrating that the spatial and laminar distribution of cartilage relaxation time maps pixels could be more sensitive than full-thickness mean values in detecting the compositional variation of cartilage [11–13].

Textural analysis (TA) offers an alternative method to examine the spatial distribution of pixel values and quantify the heterogeneity in an image. This is a statistical image analysis technique aiming to quantify the texture of an image on the basis of pixel signal intensity distributions and the relationships between values of neighbouring pixels [14]. Recent studies

have demonstrated the feasibility of characterizing the spatial distribution of cartilage T2 and T1rho using TA [8, 13, 15]. As a novel image analysis technique, TA has been applied to assess longitudinal changes, symptomatic OA, cartilage lesions, subjects at risk for OA, and degeneration following anterior cruciate ligament injury. However, it has not been used as a method for assessment longitudinal of repair cartilage with treatment of stem cells.

The objective of this study was to determine the feasibility of TA as a MR method to examine the spatial distribution of pixel values and detect the compositional variation of repair cartilage with treatment of allogeneic human adipose-derived mesenchymal progenitor cells (haMPCs).

2. Materials And Methods

Patients

Twenty-two patients with knee OA participated a phase I/IIa clinical trial (Clinicaltrials, NCT02641860. Registered 3 December 2015 at Ren Ji Hospital, School of Medicine, Shanghai Jiao Tong University, in China). Four patients were not included due to loss of follow-up. Finally, eighteen patients were divided randomly into three groups with intra-articular injections of haMPCs: the low-dose (1.0×10^7 cells), mid-dose (2.0×10^7 cells), and high-dose (5.0×10^7 cells) group with six patients each. Detailed inclusion and exclusion criteria, demographic and clinical information on subjects is given in our previous report [5]. Disease severity and movement symptom severity of OA were assessed using the Western Ontario and McMaster Universities Osteoarthritis Index (WOMAC) pain scale [16] as graded by a movement disorder specialist.

haMPC preparation

Human adipose-derived MSCs were obtained from three healthy donors that were subjected to allogeneic MSC transplantation and produced more cells than needed for clinical trial. The isolation and characterization of cells followed the conventional methods described in previous report [5, 17]. The details of characterization of the adipose-derived mesenchymal stem cell were also described in our previous work [5].

MRI imaging acquisition

All subjects were studied on a clinical 3T MR imaging system (Signa HDx; GE Healthcare, Milwaukee, WI, USA) with a dedicated 8-channel knee coil. Compositional MRI T1rho, T2, $T2^*$and $R2^*$ maps were calculated at 1 day before first injection to collect the base time point and 48 weeks to collect terminal point. Fat-saturated fast spin-echo T2-weighted (TR/TE = 2600 ms/68 ms) in the three orthogonal planes were acquired for screening other joint diseases. The T1rho data were obtained at four different spin lock durations (TSL = 10, 20, 30 and 50 ms) with fixed spin lock B_1 amplitude of 500 Hz. The T2 images were obtained from the multi-echo spin-echo sequence with the following parameters: TR = 1125 ms, TE = 7.6-49.6 ms (8 uniformly spaced echoes with echo spacing = 6 ms), FOV =160 × 160 mm^2, matrix resolution = 320 × 320, slice thickness = 4 mm, and number of slices = 16. The $T2^*$ (or $R2^*$) maps were obtained from the multi-echo gradient echo (GRE) sequence with the following parameters: TR = 60 ms, TE = 6.8-54.4 ms (8 uniformly spaced echoes with echo spacing = 6.8 ms), flip angle = 15°, FOV = 180 × 180 mm^2, matrix resolution = 384 × 384, slice thickness = 1.2 mm, and number of slices = 128.

Data processing

Reconstruction of MRI relaxation time maps

T1rho and T2 maps were calculated by mono-exponential fitting with the Levenberg-Marquardt algorithm on spin-lock and multi-echo spin echo images respectively. $T2^*$ and $R2^*$ ($1/T2^*$) maps were reconstructed from the magnitude gradient-echo data with auto-regression on linear operations (ARLO), a mono exponential fitting method suitable for short echo time such as cartilage [18]. All reconstructions were implemented on MATLAB 2016a (MathWorks, MA, USA).

Regions of Interest Measurement

Regions of interest (ROIs) were manually traced on the high-resolution fat suppressed T2-weighted images, more obvious image of cartilage boundary, using MRIcro software (www.micro.com) by two radiologists who were blinded to subject age, disease status, and demographics. Six ROIs were defined as shown in Fig. 1: posterior lateral femoral condyle (pLFC), posterior medial femoral condyle (pMFC), trochlea lateral femur (trLF), trochlea medial femur (trMF), lateral patellar (LP), central patellar (CP), and medial patellar (MP). To maintain quantitative accuracy, the ROIs drawn on the fat suppressed T2-weighted images were applied to relaxation time maps. Voxels at the tissue boundaries were also excluded.

3D Texture analysis based on gray level run-length matrix

3D texture analyses based gray level run-length matrix (GLRLM) of the segmented ROIs were conducted using MaZda software (http://www.eletel.p.lodz.pl/programy/mazda/, Lodz, Poland) as MacKay's report [19]. The GLRLM p (i, j) searches the image in a given direction for runs of pixels having the same grey-level value. The matrix element (i, j) represents the number of times the image contains pixels having gray level i and run of length j in the given direction. The current study focused on a set of higher-order statistics features obtained from the GLRLM: run length non-uniformity (RLNonUni), grey level non-uniformity (GLevNonU), long run emphasis (LngREmph), short run emphasis (ShrtREmp) and fraction of image in runs (Fraction). Descriptions and equations of each texture feature are summarized in Table 1. The MaZda parameters were: 8 bits per pixel, and the distance between a pair of voxels for GLRLM features was 1 voxel. The GLRLM parameters were computed 4 times for each ROI (for vertical, horizontal, 45-degree and 135-degree directions) as shown in Fig. 2. The mean value of each GLRLM parameter for each pixel in all possible directions and pixel offsets was calculated for each coronal image. GLRLM features were calculated 20 times for each pixel at a variety of pixel offsets ranging from 1 to 5 pixels. The values of each texture parameter on each of the four relaxation time constant mappings analysed were then averaged to give summary values in each participant for cartilage ROIs.

Statistical analyses

Statistical analyses were carried out using SPSS for Windows version 23.0 (IBM SPSS Statistics, Chicago, IL). The differences between the three dose groups were compared using one-way analysis of variance (ANOVA), followed by Tukey's multiple comparison test undertaken when significant differences in means were observed. We used the difference before and after treatment (D values) as the object to avoid errors caused by individual differences. Changes from base time in all measures that were scale variables were determined with a paired t-test (two-tailed) followed by Mann-Whitney U tests. Two-tailed Pearson linear correlation analysis was used to investigate correlations between texture parameters and the WOMAC scores. Inter-observer segmentation variability was tested using the intra-class correlation coefficient (ICC) for the two researchers. An ICC of 0.81–1.00 was considered to indicate excellent agreement; 0.61 to 0.80 for good agreement; 0.41 to 0.60 for moderate agreement; 0.21 to 0.40 for fair agreement; and 0.20 or less for poor agreement. A *P* value of less than 0.05 was considered statistically significant.

3. Results

(1) Test-retest reliability analysis

Test-retest reliability of manual ROI extraction by two researchers was evaluated using ICC analysis. The ICC value for absolute agreement between the two researchers with respect to cartilage voxel volume was 0.85, indicating excellent inter-observer agreement. Given the excellent agreement between the two researchers, the results of the texture analyses were the average of the two researchers' measurements.

(2) multiple comparison of three dose groups

The heterogeneity of spatial distribution of pixels from three groups was decreased to varying degrees at 48 weeks after intra-articular injection of haMPCs (Fig. 3). Spatial distribution of cartilage relaxation time maps pixels were uneven and layered, especially in T2 maps (Fig. 3b). Compared with base time, there were significant differences among three dose

groups in GLRLM features for T1rho map including RLNonUni (F = 23.705, P < 0.0001), GLevNonU (F = 24.888, P < 0.0001), LngREmph (F = 14.916, P = 0.0003), for T2 map including LngREmph (F = 7.867, P = 0.005), GLevNonU (F = 9.461, P = 0.002), ShrtREmp (F = 8.673, P = 0.003), for $T2^*$ map including RLNonUni (F = 3.961, P = 0.042), GLevNonU (F = 7.953, P = 0.004), and for $R2^*$ map including RLNonUni (F = 5.785, P = 0.014), GLevNonU (F = 3.833, P = 0.045) (Fig. 4 & Table 2). The significant differences of GLRLM features of MRI relaxation time maps demonstrated texture analysis method be potential to distinguish each group with different dose of haMPCs.

(3) The correlations between GLRLM features and clinical pain scores.

WOMAC pain scores were associated with RLNonUni of T1rho map (R^2 = 0.347, P = 0.031), GLevNonU of T2 map (R^2 = 0.366, P = 0.028), LngREmph of $T2^*$ map (R^2 = -0.367, P = 0.028), LngREmph of $R2^*$ map (R^2 = -0.356, P = 0.033) and Fraction of T1rho map (R^2 = 0.36, P = 0.033), whereas no significant correlations in other measurements (Fig. 5).

4. Discussion

In recent decades, allogeneic MSC/MPCs were demonstrated to repair the damaged articular cartilage due to their greater feasibility and lack of serious adverse effects [20–23]. The efficacy of intra-articular injection of haMPCs in the knee has been verified in OA animal models [17] and patients in our previous phase I/IIa clinical trial [5]. We quantified the spatial relations of cartilage components by 3D texture analysis of MRI relaxation times, combined with clinical outcomes, to evaluate the relationship of texture parameters of MRI relaxation time maps and compositional variation of repair cartilage with this treatment. This study highlights the complex interactions between the various repaired tissues with treatment of haMPCs, and suggests that cartilage biochemical composition may play an integral role in the progression of morphologic disease.

Articular cartilage is divided into four zones termed as superficial, intermediate, deep, and calcified layer from the joint surface to the underlying bone. The molecular orientation and distribution of PGs and GAGs in the collagen network are different in four zones of the ECM [7, 24]. MSC/MPCs show different abilities of regeneration and differentiation to restore the degeneration of ECM in different zones [25]. Texture features might show detailed information of repair ability of MSC/MPCs in different zones by providing unique information on the spatial heterogeneity of the cartilage, that are otherwise not readily apparent using conventional mean measurements of MRI maps. 3D texture analysis based on GLRLM features, are higher-order descriptors of the spatial organization of pixels in ROIs by measuring the distributions and sizes of areas (groups of pixels) within the ROIs having the same gray-level values. Recent studies reporting texture analysis of cartilage heterogeneity used histogram analysis and grey level co-occurrence matrix (GLCM) [4, 15, 26] to obtain results. Compared with GLCM, the GLRLM features performed better in the optimal subset and more sensitive to variation of regional heterogeneity because it analyses texture changes through the entire length of the run, and less dependent on the distribution range of pixel values in the image because the pixel values as well as the lengths of the same pixel values are considered together for GLRLM assessments [27].

In our study, most GLRLM textural features were significantly different between the three groups, especially in T2 and T1rho maps, including RLNonUni, LngREmph and ShrtREmp, suggesting a possible changes of spatial distribution in cartilage composition with this treatment (Fig. 3a-b & Fig. 4). The heterogeneity of spatial distribution of pixels from three groups was decreased to varying degrees at 48 weeks after intra-articular injection of haMPCs. This result was consistent with recent studies that suggested the uniformity of both T1rho and T2 maps pixels represented, to a certain extent, the change of cartilage composition [13]. In principle, GLRLM textural features showed different interactions with surrounding water molecules between different layers of cartilage for T2 maps [28], and showed differential maturation of the repair tissue for its GAG and collagen specificity between layers for T1rho maps [29]. Although further work is needed to elucidate the different mechanisms that contribute to T1rho and T2 relaxations in different zones of cartilage, we hypothesize that GLRLM textural features of these two MRI relaxation time parameters may provide complementary information regarding macromolecular changes in cartilage.

GLevNonU measures the similarity of grey level intensity values in the image. High GLevNonU values represent a non-uniform texture, i.e., heterogeneity, where a lower GLevNonU value correlates with a greater similarity in intensity values [30]. In current study, GLevNonU values of T2 maps, were correlated with WOMAC pain scores as shown in Fig. 5b (R^2 = 0.366, P = 0.028), whereas no correlation was found in GLevNonU values of other relaxation maps. This result was consistent with Carballido's demonstration that the uniformity of cartilage T2 map is affected by disease [7]. Compared with mean measurements of whole cartilage [5], GLevNonU values of T2 maps might be potential to evaluate the efficacy of different doses of haMPCs more precisely.

The correlations between WOMAC pain scores and texture parameters as shown Fig. 5 demonstrated the spatial heterogeneity of relaxation time maps maybe associated with clinical scores, whereas no such correlation was found in the mean relaxation values in our previous study [5]. This was consistent with Joseph's conclusion that the heterogeneous nature of cartilage tissue, compared with mean values, is more important consideration when quantifying cartilage tissue integrity [15].

No significant difference was found in LngREmph of $T2^*$ (the reciprocal of $R2^*$) or $R2^*$ in three groups (Table 2 & Fig. 4c). The result was consistent with our previous conclusion that $T2^*$ (or $R2^*$) mapping was less sensitive than other mapping (such as T1rho and T2 mapping) in differentiating difference between three dose groups [5]. The current research is novel, however, in its investigation of the significant negative correlation between $T2^*$ (or $R2^*$) and LngREmph (Fig. 5c). Crema et al reported an association between $T2^*$ values and the local field inhomogeneities and susceptibility, caused by changes of restricted water mobility in the ECM [31]. The results of the current study are consistent with Crema's report, highlighting an interaction between cartilage biochemical composition and $T2^*$ texture parameters. Considering the inhomogeneous distribution of $T2^*$ pixels, texture parameters of $T2^*$ and $R2^*$ maps, especially RLNonUni and GLevNonU, maybe more potential to detection of the compositional variation of cartilage composition than the mean value, considering the inhomogeneous distribution of susceptibility in layered structure of cartilage in maps.

This study builds on our previous work repairing cartilage with allogeneic haMPCs and will aid future research in this area with regard to selection of MRI texture features most likely to be most useful, taking into account discriminatory ability, reliability, and relationship to clinical pain scores.

Our study had several limitations. Firstly, the number of subjects was relatively small, so there is a need to encourage large randomized clinical trials for texture analysis. Secondly, we should implement comprehensive texture analysis, not just GLRLM (third-order) texture analysis, although it has more advantages on the distribution range of pixel values in the image than first-order and second-order texture analysis. Thirdly, we used conventional texture analysis parameters without considering that heterogeneity increases as the number of pixels showing a large difference from adjacent pixels increases. Finally, no histological analysis was supplemented. The histological data should be confirmed in future studies to provide direct evidence of the heterogeneity of spatial distribution of pixels of relaxation maps.

5. Conclusion

MRI texture analysis of cartilage may allow detection of the compositional variation of repair cartilage with treatment of allogeneic haMPCs. This has potential applications in understanding mechanism of stem cells repairing cartilage and assessing response to treatment.

Abbreviations

MSC/MPC
mesenchymal stem/progenitor cells
haMPCs
human adipose-derived MPCs

MRI
Magnetic resonance imaging
OA
osteoarthritis
PG
proteoglycan
GAG
glycosaminoglycan
ECM
extracellular matrix
ROI
region of interest
TA
Textural analysis
WOMAC
Western Ontario and McMaster Universities Osteoarthritis Index
ARLO
auto-regression on linear operations
pLFC
posterior lateral femoral condyle
pMFC
posterior medial femoral condyle
trLF
trochlea lateral femur
trMF
trochlea medial femur
LP
lateral patellar
CP
central patellar
MP
medial patellar
GLRLM
gray level run-length matrix
RLNonUni
run length non-uniformity
GLevNonU
grey level non-uniformity
LngREmph
long run emphasis
ShrtREmp
short run emphasis
Fraction
fraction of image in runs
ANOVA
analysis of variance
ICC

intraclass correlation coefficient

GLCM

grey level co-occurrence matrix

Declarations

Ethics approval and consent to participate

All methods were carried out in accordance with relevant guidelines and regulations. All experimental protocols were approved by the ethics committee of Renji Hospital Affiliated to Medical College of Shanghai Jiaotong University (Shanghai, China).

Consent for publication

Not applicable.

Availability of data and material

The datasets used and/or analyzed during the current study are available from the corresponding author upon request.

Competing interest

There is no conflict of interest of all the authors.

Funding

This work was supported by the Shanghai Municipal Population and Family Planning Commission (Grant No. 20194Y0087) and National Natural Science Foundation of China (#8190070095).

Authors' contributions

XZ analyzed and interpreted the data, prepared all figures, drafted the manuscript, and revised it; QL and JR collected the data and provided technical assistance; JL and CD polished the language of the article and made some pertinent proposal on the scheme; MP and YZ designed the study, revised the manuscript critically for important intellectual content, and approved the final version to be submitted. All authors contributed to the data interpretation and manuscript preparation. All authors approved the final submitted submission.

Acknowledgements

We express our sincere appreciation to the patients who participated in this trial. We thank Cellular Biomedicine Group for providing adipose-derived mesenchymal progenitor cells. Cellular Biomedicine Group did not in any way try to suppress information or influence the conclusions of the study authors.

References

1. Pas HI, Winters M, Haisma HJ, Koenis MJ, Tol JL, Moen MH. Stem cell injections in knee osteoarthritis: a systematic review of the literature. Br J Sports Med. 2017;51:1125–1133. doi:10.1136/bjsports-2016-096793.
2. Gupta PK, Das AK, Chullikana A, Majumdar AS. Mesenchymal stem cells for cartilage repair in osteoarthritis. Stem Cell Res Ther. 2012;3:25. doi:10.1186/scrt116.
3. Wolfstadt JI, Cole BJ, Ogilvie-Harris DJ, Viswanathan S, Chahal J. Current concepts: the role of mesenchymal stem cells in the management of knee osteoarthritis. Sports Health. 2015;7:38–44. doi:10.1177/1941738114529727.

4. Joseph GB, Baum T, Alizai H, Carballido-Gamio J, Nardo L, Virayavanich W *et al.* Baseline mean and heterogeneity of MR cartilage T2 are associated with morphologic degeneration of cartilage, meniscus, and bone marrow over 3 years–data from the Osteoarthritis Initiative. Osteoarthritis Cartilage. 2012;20:727–735. doi:10.1016/j.joca.2012.04.003.
5. Zhao X, Ruan J, Tang H, Li J, Shi Y, Li M *et al.* Multi-compositional MRI evaluation of repair cartilage in knee osteoarthritis with treatment of allogeneic human adipose-derived mesenchymal progenitor cells. Stem Cell Res Ther. 2019;10:308. doi:10.1186/s13287-019-1406-7.
6. Guermazi A, Alizai H, Crema MD, Trattnig S, Regatte RR, Roemer FW. Compositional MRI techniques for evaluation of cartilage degeneration in osteoarthritis. Osteoarthritis Cartilage. 2015;23:1639–1653. doi:10.1016/j.joca.2015.05.026.
7. Carballido-Gamio J, Stahl R, Blumenkrantz G, Romero A, Majumdar S, Link TM. Spatial analysis of magnetic resonance T1rho and T2 relaxation times improves classification between subjects with and without osteoarthritis. Med Phys. 2009;36:4059–4067. doi:10.1118/1.3187228.
8. Blumenkrantz G, Stahl R, Carballido-Gamio J, Zhao S, Lu Y, Munoz T *et al.* The feasibility of characterizing the spatial distribution of cartilage T(2) using texture analysis. Osteoarthritis Cartilage. 2008;16:584–590. doi:10.1016/j.joca.2007.10.019.
9. Carballido-Gamio J, Blumenkrantz G, Lynch JA, Link TM, Majumdar S. Longitudinal analysis of MRI T(2) knee cartilage laminar organization in a subset of patients from the osteoarthritis initiative. Magn Reson Med. 2010;63:465–472. doi:10.1002/mrm.22201.
10. Welsch GH, Mamisch TC, Domayer SE, Dorotka R, Kutscha-Lissberg F, Marlovits S *et al.* Cartilage T2 assessment at 3-T MR imaging: in vivo differentiation of normal hyaline cartilage from reparative tissue after two cartilage repair procedures–initial experience. Radiology. 2008;247:154–161. doi:10.1148/radiol.2471070688.
11. Carballido-Gamio J, Joseph GB, Lynch JA, Link TM, Majumdar S. Longitudinal analysis of MRI T2 knee cartilage laminar organization in a subset of patients from the osteoarthritis initiative: a texture approach. Magn Reson Med. 2011;65:1184–1194. doi:10.1002/mrm.22693.
12. Hauser N, DiCesare PE, Paulsson M. The spatial and temporal expression of cartilage matrix protein illustrates the molecular heterogeneity of cartilage. Acta Orthop Scand Suppl. 1995;266:19–21.
13. Li X, Pai A, Blumenkrantz G, Carballido-Gamio J, Link T, Ma B *et al.* Spatial distribution and relationship of T1rho and T2 relaxation times in knee cartilage with osteoarthritis. Magn Reson Med. 2009;61:1310–1318. doi:10.1002/mrm.21877.
14. MacKay JW, Murray PJ, Kasmai B, Johnson G, Donell ST, Toms AP. MRI texture analysis of subchondral bone at the tibial plateau. Eur Radiol. 2016;26:3034–3045. doi:10.1007/s00330-015-4142-0.
15. Joseph GB, Baum T, Carballido-Gamio J, Nardo L, Virayavanich W, Alizai H *et al.* Texture analysis of cartilage T2 maps: individuals with risk factors for OA have higher and more heterogeneous knee cartilage MR T2 compared to normal controls–data from the osteoarthritis initiative. Arthritis Res Ther. 2011;13:R153. doi:10.1186/ar3469.
16. Hayashi D, Guermazi A, Kwoh CK. Clinical and translational potential of MRI evaluation in knee osteoarthritis. Curr Rheumatol Rep. 2014;16:391. doi:10.1007/s11926-013-0391-6.
17. Wang W, He N, Feng C, Liu V, Zhang L, Wang F *et al.* Human adipose-derived mesenchymal progenitor cells engraft into rabbit articular cartilage. Int J Mol Sci. 2015;16:12076–12091. doi:10.3390/ijms160612076.
18. Pei M, Nguyen TD, Thimmappa ND, Salustri C, Dong F, Cooper MA *et al.* Algorithm for fast monoexponential fitting based on Auto-Regression on Linear Operations (ARLO) of data. Magn Reson Med. 2015;73:843–850. doi:10.1002/mrm.25137.
19. MacKay JW, Kapoor G, Driban JB, Lo GH, McAlindon TE, Toms AP *et al.* Association of subchondral bone texture on magnetic resonance imaging with radiographic knee osteoarthritis progression: data from the Osteoarthritis Initiative Bone Ancillary Study. Eur Radiol. 2018;28:4687–4695. doi:10.1007/s00330-018-5444-9.
20. Lee KB, Hui JH, Song IC, Ardany L, Lee EH. Injectable mesenchymal stem cell therapy for large cartilage defects--a porcine model. Stem Cells. 2007;25:2964–2971. doi:10.1634/stemcells.2006-0311.
21. Sordi V. Mesenchymal stem cell homing capacity. Transplantation. 2009;87:S42-45. doi:10.1097/TP.0b013e3181a28533.

22. Agung M, Ochi M, Yanada S, Adachi N, Izuta Y, Yamasaki T *et al.* Mobilization of bone marrow-derived mesenchymal stem cells into the injured tissues after intraarticular injection and their contribution to tissue regeneration. Knee Surg Sports Traumatol Arthrosc. 2006;14:1307–1314. doi:10.1007/s00167-006-0124-8.
23. Kantake M, Hirano A, Sano M, Urushihata N, Tanemura H, Oki K *et al.* Transplantation of allogeneic adipose-derived mesenchymal stem cells in a cerebral palsy patient (Retracted). Regen Med. 2017;12:575. doi:10.2217/rme-2017-0043.
24. Welsch GH, Mamisch TC, Quirbach S, Zak L, Marlovits S, Trattnig S. Evaluation and comparison of cartilage repair tissue of the patella and medial femoral condyle by using morphological MRI and biochemical zonal T2 mapping. Eur Radiol. 2009;19:1253–1262. doi:10.1007/s00330-008-1249-6.
25. Jo CH, Lee YG, Shin WH, Kim H, Chai JW, Jeong EC *et al.* Intra-articular injection of mesenchymal stem cells for the treatment of osteoarthritis of the knee: a proof-of-concept clinical trial. Stem Cells. 2014;32:1254–1266. doi:10.1002/stem.1634.
26. Mayerhoefer ME, Welsch GH, Riegler G, Mamisch TC, Materka A, Weber M *et al.* Feasibility of texture analysis for the assessment of biochemical changes in meniscal tissue on T1 maps calculated from delayed gadolinium-enhanced magnetic resonance imaging of cartilage data: comparison with conventional relaxation time measurements. Invest Radiol. 2010;45:543–547. doi:10.1097/RLI.0b013e3181ea363b.
27. Brunese L, Mercaldo F, Reginelli A, Santone A. Radiomics for Gleason Score Detection through Deep Learning. Sensors (Basel). 2020;20. doi:10.3390/s20185411.
28. Dardzinski BJ, Mosher TJ, Li S, Van Slyke MA, Smith MB. Spatial variation of T2 in human articular cartilage. Radiology. 1997;205:546–550. doi:10.1148/radiology.205.2.9356643.
29. Holtzman DJ, Theologis AA, Carballido-Gamio J, Majumdar S, Li X, Benjamin C. T(1rho) and T(2) quantitative magnetic resonance imaging analysis of cartilage regeneration following microfracture and mosaicplasty cartilage resurfacing procedures. J Magn Reson Imaging. 2010;32:914–923. doi:10.1002/jmri.22300.
30. Traverso A, Wee L, Dekker A, Gillies R. Repeatability and Reproducibility of Radiomic Features: A Systematic Review. Int J Radiat Oncol Biol Phys. 2018;102:1143–1158. doi:10.1016/j.ijrobp.2018.05.053.
31. Crema MD, Roemer FW, Marra MD, Burstein D, Gold GE, Eckstein F *et al.* Articular cartilage in the knee: current MR imaging techniques and applications in clinical practice and research. Radiographics. 2011;31:37–61. doi:10.1148/rg.311105084.

Tables

Table 1

Description and equation of eleven second order texture parameters based on run-length matrix (GLRLM).

Feature	Description	Equation
RLNonUni	run length non-uniformity	$\frac{\sum_{j=1}^{N_r}(\sum_{i=1}^{N_g} p(i,j))^2}{C}$
GLevNonU	grey level non-uniformity	$\frac{\sum_{i=1}^{N_g}(\sum_{j=1}^{N_r} p(i,j))^2}{C}$
LngREmph	long run emphasis	$\frac{\sum_{i=1}^{N_g}\sum_{j=1}^{N_r} j^2 p(i,j)}{C}$
ShrtREmp	short run emphasis	$\frac{\sum_{i=1}^{N_g}\sum_{j=1}^{N_r} \frac{p(i,j)}{j^2}}{C}$
Fraction	fraction of image in runs	$\frac{\sum_{i=1}^{N_g}\sum_{j=1}^{N_r} p(i,j)}{\sum_{i=1}^{N_g}\sum_{j=1}^{N_r} jp(i,j)}$

Note: The GLRLM element p (i, j) reflects the probability of a pair of gray values i and j in a specified spatial displacement of an image; Ng represents the number of grey levels and Nr represents the number of runs.

Table 2

The results of D value analysis of texture parameters and multiple comparison of three dose groups.

Relaxation maps	Features	High	Mid	Low	*F* value (Multiple comparison)	*P* value (Multiple comparison)	*P* value (High vs Mid)	*P* value (High vs Low)	*P* value (Mid vs Low)
T1rho (ms)	RLNonUni	3.51 ± 0.44	2.85 ± 0.56	0.51 ± 0.05	23.705	<0.0001***	0.170	<0.0001***	0.0001***
	GLevNonU	10.12 ± 1.71	8.01 ± 1.91	1.32 ± 0.37	24.888	<0.0001***	0.127	<0.0001***	0.0001***
	LngREmph	13.42 ± 0.40	5.78 ± 0.31	4.02 ± 0.34	14.916	0.0003***	0.001**	0.0001***	0.352
	ShrtREmp	0.07 ± 0.002	0.05 ± 0.003	0.02 ± 0.008	1.679	0.220	0.490	0.089	0.284
	Fraction	0.05 ± 0.02	0.04 ± 0.01	0.03 ± 0.003	0.193	0.826	0.825	0.548	0.702
T2 (ms)	RLNonUni	4.87 ± 0.27	1.78 ± 0.16	0.83 ± 0.07	7.867	0.005**	0.011*	0.002**	0.388
	GLevNonU	1.80 ± 0.21	6.26 ± 0.34	9.00 ± 0.32	9.461	0.002**	0.018*	0.001**	0.111
	LngREmph	27.20 ± 0.21	16.20 ± 2.44	8.80 ± 0.68	3.078	0.076	0.160	0.026*	0.340
	ShrtREmp	0.10 ± 0.002	0.02 ± 0.003	0.01± 0.002	8.673	0.003**	0.003**	0.002**	0.927
	Fraction	0.02 ± 0.006	0.03 ± 0.002	0.06 ± 0.002	2.856	0.089	0.852	0.048*	0.068
$T2^*$ (ms)	RLNonUni	1.58 ± 0.05	1.10 ± 0.01	1.02 ± 0.07	3.961	0.042*	0.026*	0.030*	0.947
	GLevNonU	18.10 ± 3.32	15.90 ± 3.16	11.50 ± 2.47	7.953	0.004**	0.277	0.001**	0.015*
	LngREmph	33.50 ± 1.59	31.15 ± 1.15	24.7 ± 1.81	1.235	0.058	0.217	0.894	0.175
	ShrtREmp	0.02 ± 0.004	0.03 ± 0.003	0.02 ± 0.005	3.451	0.058	0.024*	0.550	0.076
	Fraction	0.02 ± 0.006	0.03 ± 0.003	0.03 ± 0.005	2.720	0.098	0.148	0.037*	0.457
$R2^*$ (s^{-1})	RLNonUni	1.58 ± 0.57	1.70 ± 0.21	1.12 ± 0.46	5.785	0.014*	0.519	0.022*	0.006**

	GLevNonU	2.11 ± 0.11	4.35 ± 0.18	5.63 ± 0.36	3.833	0.045*	0.102	0.015*	0.335
	LngREmph	27.25 ± 3.42	29.93 ± 5.21	24.73 ± 1.80	0.409	0.672	0.648	0.667	0.380
	ShrtREmp	0.02 ± 0.003	0.04 ± 0.002	0.03 ± 0.006	0.468	0.635	0.359	0.527	0.027*
	Fraction	0.11 ± 0.008	0.08 ± 0.010	0.03 ± 0.006	3.115	0.074	0.429	0.122	0.027*

* $P < 0.05$, ** $P < 0.01$, *** $P < 0.001$

Figures

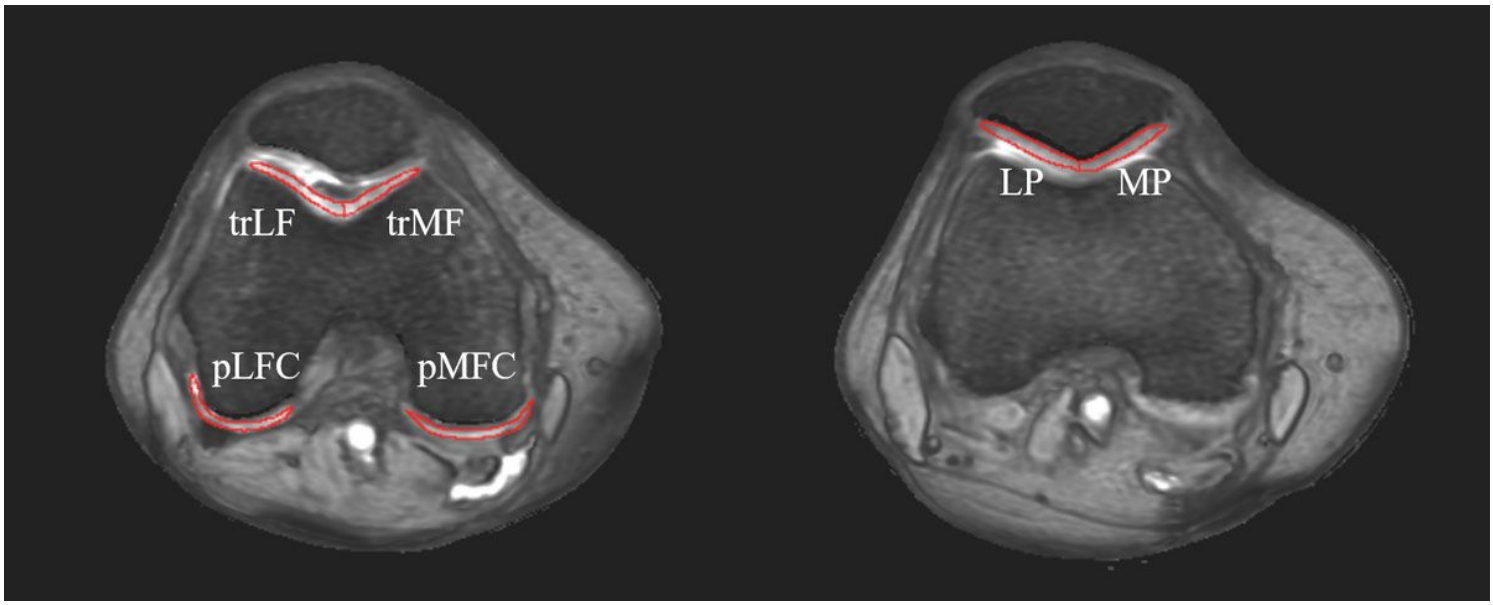

Figure 1

Definition of regions of interest of cartilage on transverse fat suppressed T2-weighted images. trLF: lateral side of trochlea; trMF: medial side of trochlea; LFC: lateral femoral condyle; MFC: medial femoral condyle; LP: lateral side of patella; MP: medial side of patella.

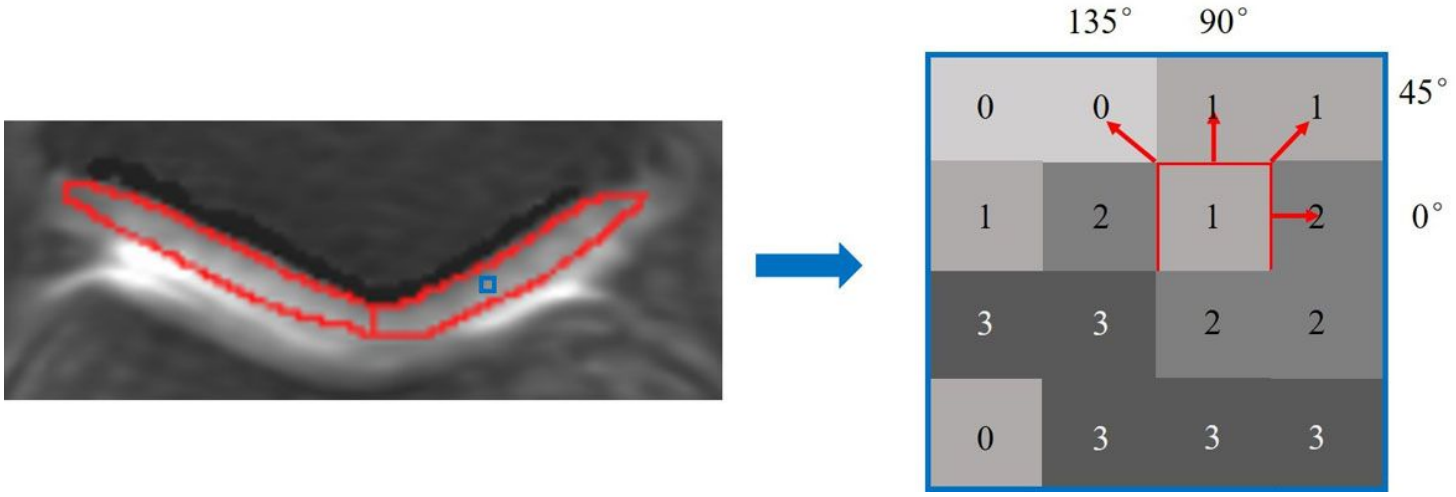

Figure 2

Illustration of the process to generate gray level run-length matrices considering a 4 * 4 image represented with four gray-tone values from 0 to 3. We considered one neighboring pixel (d = 1) along four possible directions as 0°, 45°, 90° and 135°.

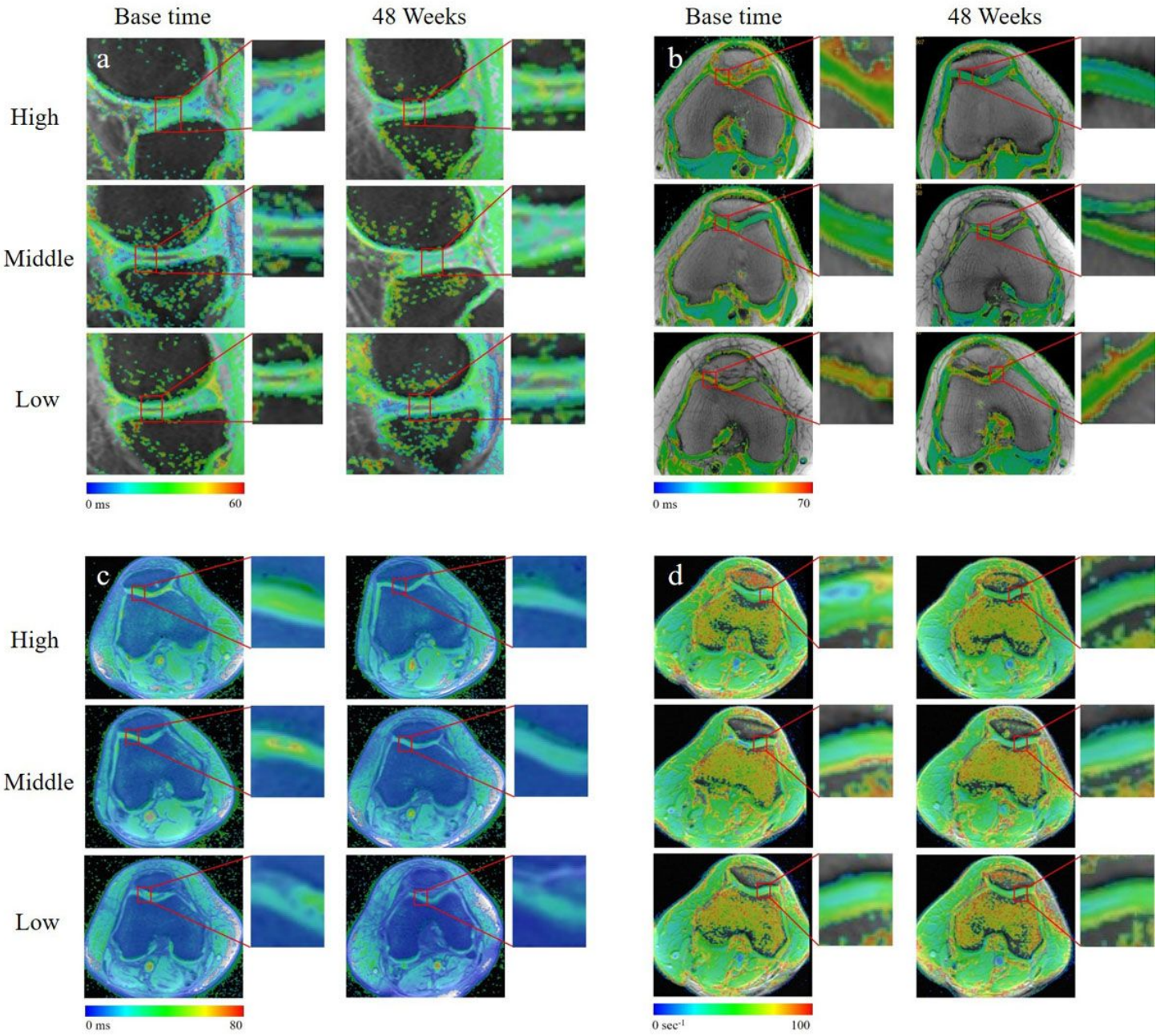

Figure 3

Representative images of quantitative MRI relaxation maps of three patients from high (60 years, F), middle (68 years, M) and low (65 years, M) dose groups. Compared with baseline, the heterogeneity of spatial distribution of pixels from three groups was decreased to varying degrees at 48 weeks after intra-articular injection of haMPCs. Spatial distribution of cartilage relaxation time maps pixels were uneven and layered (red box), especially in T2 map. T1rho (a), T2 (b), $T2^*$ (c), $R2^*$ (d).

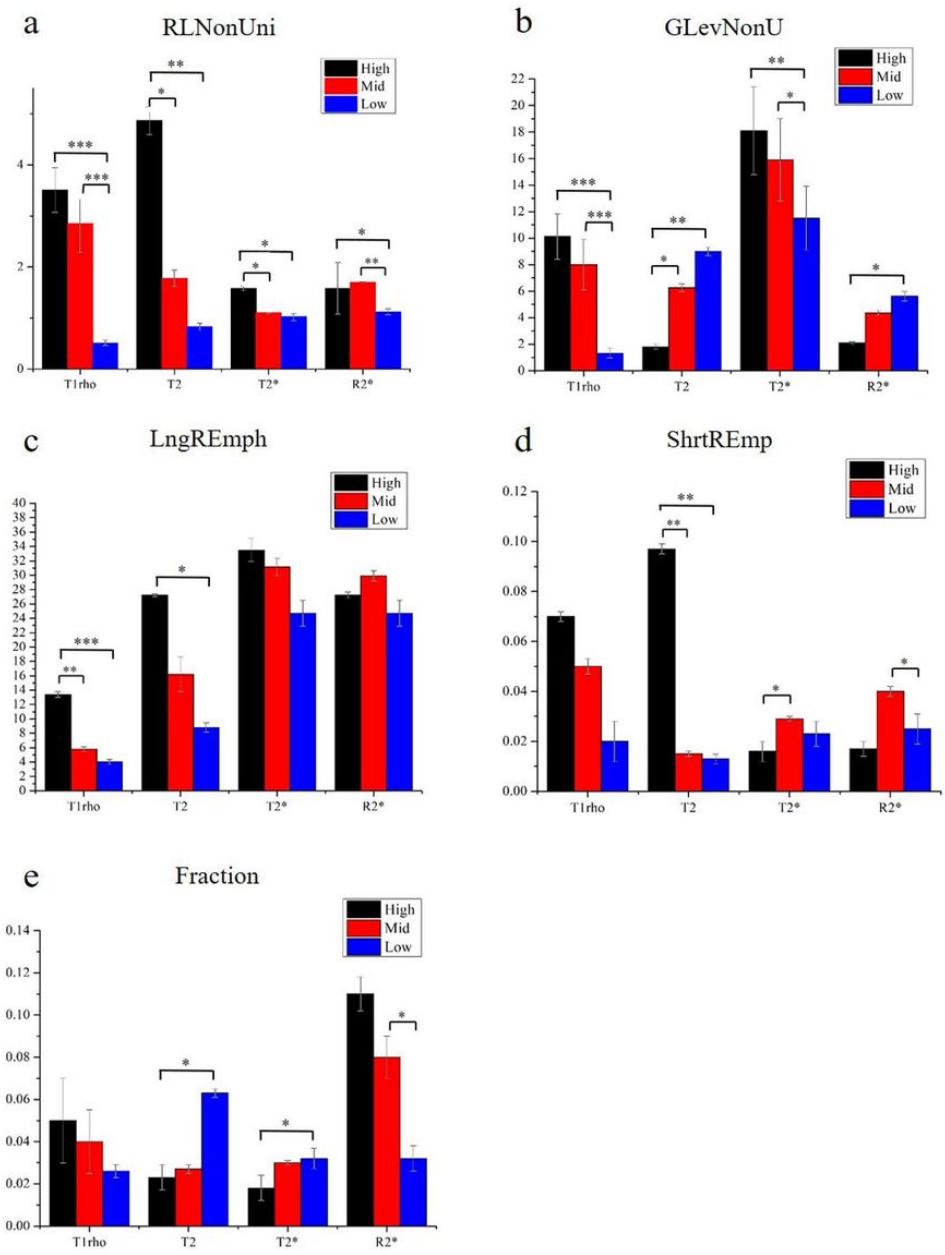

Figure 4

Comparison of texture parameters D values of MR relaxation time maps in the articular cartilage of three dose groups. RLNonUni (a): length non-uniformity; GLevNonU (b): grey level non-uniformity; LngREmph (c): long run emphasis; ShrtREmp (d): short run emphasis; Fraction (e): fraction of image in runs. * indicates P<0.05, ** indicates P<0.001, *** indicates P<0.0001.

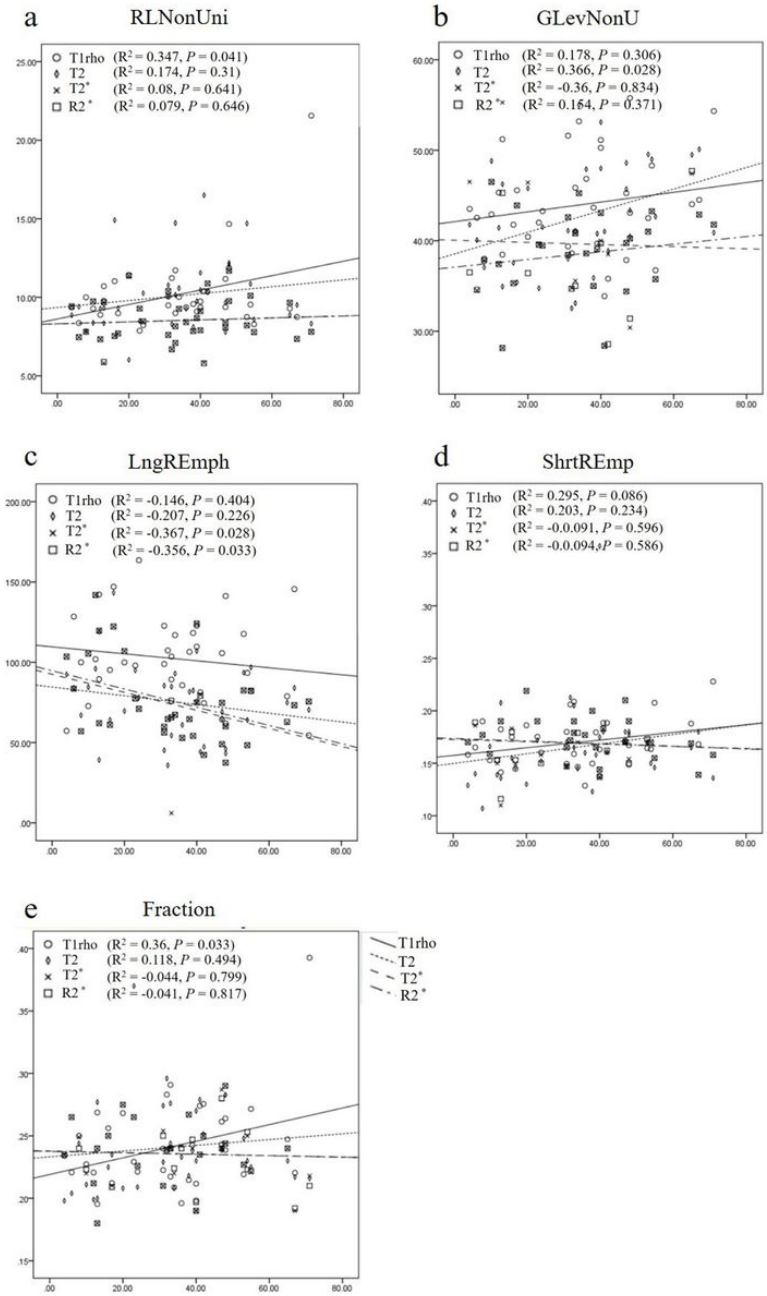

Figure 5

Correlations between WOMAC pain scores and texture parameters of MR relaxation time maps. The abscissa represents WOMAC scores. RLNonUni (a): length non-uniformity; GLevNonU (b): grey level non-uniformity; LngREmph (c): long run emphasis; ShrtREmp (d): short run emphasis; Fraction (e): fraction of image in runs.